9528 *Macromolecules* **2009**, *42*, 9528–9536
DOI: 10.1021/ma901516v

Macromolecules
ARTICLE

Small Angle Neutron Scattering from the Highly Interacting Polymer Mixture TMPC/PSd: No Evidence of Spatially Dependent χ Parameter

João T. Cabral* and Julia S. Higgins

Department of Chemical Engineering, Imperial College, London SW7 2AZ, U.K.

Received July 13, 2009; Revised Manuscript Received November 8, 2009

ABSTRACT: We study the thermodynamics and chain dimensions of a highly interacting polymer mixture, poly(tetramethyl bisphenol A polycarbonate) and deuterated polystyrene (TMPC/PSd), using small angle neutron scattering (SANS). The one-phase region of the phase diagram is investigated as a function of blend composition ϕ and temperature T, employing three SANS diffractometers and covering a wide scattering wavevector window ($0.008 < q < 0.25$ Å^{-1}). We find that the random phase approximation (RPA), accounting for component polydispersity, describes remarkably well all scattering data. Previous SANS measurements suggested anomalous mean-field behavior of TMPC/PSd, associated with a spatially dependent or "structured" Flory interaction parameter $\chi(q)$. We show that structure factors from mixtures undergoing temperature jumps or quenched below the glass transition exhibit the same apparent deviations from RPA, suggesting that incomplete equilibration could account for the observations. After demonstrating the regular RPA behavior of TMPC/PSd, the only miscible polystyrene and polycarbonate pair, we determine for the first time comprehensive mixture interaction parameters $\chi(\phi,T)$ and the chain segment length for TMPC.

I. Introduction

Polymer miscibility is both theoretically and industrially relevant.[1,2] The interactions between macromolecules are generally understood in terms of the Flory−Huggins (FH) lattice theory[3−5] (and its improvements[6−8]) and correlation functions derived from de Gennes mean-field random phase approximation (RPA).[9] FH theory provides a description of the free energy of mixing, introducing a thermodynamic interactionparameter χ, and allowing for the computation of phase boundaries. RPA theory relates the structure factor of single-phase mixtures, measurable in a scattering experiment, to component chain dimensions and interaction χ. Small-angle neutron scattering (SANS) and RPA have been successfully employed for decades in the characterization of polymer conformation and interactions in mixtures of distinct and isotopic homopolymers and copolymers.[10]

This work is motivated in part by a controversial report of deviation from mean-field behavior observed in a mixture of poly(tetramethyl bisphenol A polycarbonate) and deuterated polystyrene (TMPC/PSd).[11] TMPC and PS, depicted in Figure 1, form partially miscible blends, exhibiting a near-symmetric lower-critical solution temperature (LCST) phase diagram with critical composition near 50/50 (weight fraction) and critical temperature near 240 °C.[12−20]

A comparative SANS study by Brereton, Fischer, and coworkers[11] of several polymer blends, including the well-known poly(vinyl methyl ether)/polystyrene (PVME/PSd), identified an anomalous temperature dependence of the structure factor of TMPC/PSd. The deviations from mean-field predictions were not related to the expected crossover (to 3D Ising behavior) near the thermodynamic spinodal, which is associated with large composition fluctuations.[9,21−23] Instead, the observations motivated the introduction of a short-range spatial model for $\chi(r)$ which seemingly reconciled the experimental results with the mean-field formalism. The introduction of "structured" monomer−monomer interactions appears problematic for a thermodynamic quantity but did account for the measured data. A separate study by Yang and O'Reilly[24] reported SANS measurements of TMPC/PSd as a function of composition at constant temperature. The structure factors were satisfactorily interpreted by the RPA and the dependence of the χ parameter on composition was reported. To resolve the controversy surrounding the temperature dependence of TMPC/PSd scattering and the suitability of mean-field RPA analysis, we revisit the mixture thermodynamics by SANS.

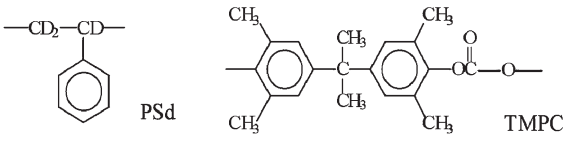

Figure 1. Monomer structures of deuterated polystyrene (PSd) and tetramethyl bisphenol A polycarbonate (TMPC).

The limited measurements available of TMPC/PSd interaction parameters, and their dependence on temperature and composition, provide the second major motivation for this work. Previous SANS reports are conflicting[11] and did not provide a description of $\chi(T,\phi)$.[24] Separately, the FRES approach to blend thermodynamics,[17,25] albeit promising, is strongly model-dependent, requires many measurable parameters (mutual and tracer diffusion coefficients, monomer friction coefficients, molecular mass distributions), and is liable to confinement and surface attraction effects characteristic of thin films, which lead to large experimental uncertainties. Small angle neutron scattering and RPA analysis remains the best established approach to describe interacting polymer mixtures in the melt[10,26] and was therefore chosen for this study of TMPC/PSd thermodynamics and chain dimensions. We determine $\chi(T,\phi)$ for an unprecedented wide temperature and composition range.

The paper is organized as follows. After introducing the TMPC/PSd blend and previous miscibility and thermodynamics

*Corresponding author. E-mail: j.cabral@imperial.ac.uk.

 Published on Web 11/17/2009

studies, section II summarizes the scattering theory for single-phase mixtures. We employ the RPA approximation, taking full account of component polydispersity. Section III describes the experimental procedure, including mixture preparation, characterization and SANS measurements on three different diffractometers. We obtain the Flory−Huggins interaction parameter $\chi(T,\phi)$, the second derivative of the free energy of mixing G'', and the correlation length of composition fluctuations ζ as a function of temperature and composition. Results for these quantities are presented in section IV. In addition, we report in section IV.B nonequilibrium measurements and propose explanations for the discrepancies observed by Brereton et al.[11] Section IV.C describes measurements and analysis of the Kratky asymptote and extraction of the components' segment length. Section V discusses the current and previous $\chi(T, \phi)$ and reconciles the findings. The last section, section VI, considers local effects in polymer mixture structure factors and concludes the paper.

II. SANS of Homogeneous Binary Mixtures

The absolute coherent scattering function of a homogeneous binary mixture in thermodynamic equilibrium is given by[10]

$$\left.\frac{1}{V}\frac{\mathrm{d}\sigma}{\mathrm{d}\Omega}(q)\right|_{\mathrm{cm}^{-1}} = N_{\mathrm{A}}\left(\frac{b_1}{v_1}-\frac{b_2}{v_2}\right)^2 S(q) \tag{1}$$

where b_1 and b_2 are the coherent scattering lengths of monomer units 1 and 2 and v_1 and v_2 their monomer molar volumes. N_A is the Avogadro number. We define a contrast factor $k \equiv N_A(b_1/v_1 - b_2/v_2)^2$, such that $I[\mathrm{cm}^{-1}] = kS(q)$.

The structure factor of the mixture, according to de Gennes' mean-field "random phase approximation" (RPA),[9] can be expressed in terms of the structure factors of each component, $S_i(q)$, and of an effective interaction parameter $\tilde{\chi}_{12}$ (dimensionless) as

$$\frac{1}{S(q)} = \frac{1}{S_1(q)} + \frac{1}{S_2(q)} - 2\frac{\tilde{\chi}_{12}}{v_0} \tag{2}$$

with component structure factors [cm^3/mol]

$$S_i(q) = \phi_i v_i \langle N_i\rangle_n \langle g_D(R_{gi}^2 q^2)\rangle_w \tag{3}$$

where $\langle N_i\rangle_n$ is the number-average degree of polymerization of component i, and ϕ_i its volume fraction. v_0 is a reference molar volume, which can be taken as the geometric mean of the components v_i, $v_0 \equiv (v_1 v_2)^{1/2}$.[27] The weight-average form factor of a polydisperse component $\langle g_D(R_{gi}^2 q^2)\rangle_w$,[28] assuming a Schultz−Zimm polydispersity distribution,[29,30] is given by

$$\langle g_D(x)\rangle_w = \frac{2}{\langle x\rangle^2}\left[\left(\frac{h}{h+x}\right)^h - 1 + x\right]$$

$$x \equiv q^2\langle R_g^2\rangle_n \equiv \frac{q^2\langle R_g^2\rangle_z}{1+2/h} \tag{4}$$

$$h = \left(\frac{M_{\mathrm{w}}}{M_{\mathrm{n}}} - 1\right)^{-1}$$

where $\langle R_g^2\rangle_n^{1/2}$ and $\langle R_g^2\rangle_z^{1/2}$ are the n- and z-average radii of gyration, related to the degree of polymerization of a Gaussian coil by

$$\langle R_g^2\rangle = \frac{\langle N\rangle a^2}{6} \tag{5}$$

where a is the statistical segment length.

Forward scattering has direct thermodynamic significance as in the zero-angle limit $\langle g_D(q \to 0)_i\rangle_w \to 1$, eq 2 yields

$$\frac{1}{S(0)} = \frac{1}{\phi_1 v_1 \langle N_1\rangle_w} + \frac{1}{\phi_2 v_2 \langle N_2\rangle_w} - 2\frac{\tilde{\chi}_{12}}{v_0} \tag{6}$$

the second derivative of the free energy of mixing with respect to composition,[9] $1/S(0) = G'' = (2/v_0)[\chi_s - \tilde{\chi}_{12}(T)]$, and

$$\chi_s = \frac{v_0}{2}\left(\frac{1}{\phi_1 v_1 \langle N_1\rangle_w} + \frac{1}{\phi_2 v_2 \langle N_2\rangle_w}\right) \tag{7}$$

is the interaction parameter at the spinodal (i.e., in the limit of thermodynamic stability, when $G'' = 0$).

The effective interaction parameter, directly measured by SANS $\tilde{\chi}_{12}$, is related to the Flory−Huggins parameter χ_{12} according to

$$\tilde{\chi}_{12} = -\frac{1}{2}\frac{\partial^2[\phi(1-\phi)\chi_{12}]}{\partial\phi^2} \tag{8}$$

where $\tilde{\chi}_{12}$ becomes equivalent to χ_{12} for composition-independent interactions.

The low-angle ($qR_g \ll 1$) scattering of thermal composition fluctuations can be described according to the Ornstein−Zernike formulation by a Lorentzian profile

$$S(q) = \frac{S(0)}{1+\xi^2 q^2} \tag{9}$$

characterizing the exponential decay of the composition fluctuations correlation function, with correlation length ξ. Equation 9 is linear in the Zimm representation as

$$1/S(q) = 1/S(0) + Aq^2 \tag{10}$$

with slope

$$A = \frac{1}{3}\left(\frac{\langle R_{g1}{}^2\rangle_z}{\phi_1 v_1 \langle N_1\rangle_w} + \frac{\langle R_{g2}{}^2\rangle_z}{\phi_2 v_2 \langle N_2\rangle_w}\right) \tag{11}$$

and $\xi \equiv [AS(0)]^{1/2}$. Given that $\chi \propto 1/T$,[31] the intercept varies as $1/S(0) \propto |1/T - 1/T_s|$ while the slope A is largely constant, since chain dimensions vary slowly with temperature. The spinodal temperature is obtained by extrapolation of the intercept to zero (or ξ to infinity) from the one-phase region. Off-critical compositions require extrapolations from outside the metastable region, to clear phase separation via nucleation and growth. In the near vicinity of the spinodal, as the length scale of concentration fluctuations diverges, a transition from a mean field behavior to a (nonmean field) Ising critical behavior is expected.[9,21] In that crossover region, $1/S(0)$ deviates from linearity with $1/T$ (resulting in a subtle slope A increase) and a new critical temperature is defined T_C.[22,23]

III. Experimental Section

A. Polymer Mixtures. Mixtures of tetramethyl bisphenol A polycarbonate (TMPC, Bayer AG)[32] and deuterated polystyrene (PSd, synthesized) were prepared by solution casting from toluene (99.8% HPLC Aldrich, 0.2 μm filtered). Sample characteristics are given in Table 1 and monomer structure in Figure 1. Glass transition temperatures T_g were determined by DSC (Perkin-Elmer Pyris 2, 10 °C/min, midpoint method) and found to be 100 and 197 °C for pure components PS and TMPC and 118 °C, 130 and 148 °C for mixtures TMPC/PS 30/70, 50/50 and 70/30 respectively.

Table 1. Sample Characterization[a]

	$\langle M\rangle_w$ (g/mol)	$\langle M\rangle_w/\langle M\rangle_n$	m (g/mol)	T_g (°C)	b_{coh} (fm)	a (Å)
PSd	225 000	1.03	112.2	100	106.54	6.7
TMPC	54 000	3.51	310.4	197	68.07	20.1

ν(PSd) = 0.061T [°C] + 94.2 [cm^3/mol] α_P(PSd, 200 °C) = 5.72×10^{-4} K^{-1}
ν(TMPC) = 0.212T [°C] + 257.9 [cm^3/mol] α_P(TMPC, 200 °C) = 7.05×10^{-4} K^{-1}
ν = 0.114T [°C] + 155.9 [cm^3/mol]

[a] Weight- and number-average degrees of polymerization, $\langle M\rangle_w$ and $\langle M\rangle_n$, were determined by GPC and given in polystyrene equivalent. m is the molecular weight of the monomer unit. Glass transition temperatures T_g were determined by DSC. b_{coh} is the neutron scattering length of the monomer units. a are the polymer segment lengths ($a(PS)$ from[37] and $a(TMPC)$ determined in this work). ν are monomer molar volumes computed from PVT data[53] [assuming ν(PSd) ≈ ν(PS)]. Reference volume was defined as $v_0 = [\nu(\text{PSd})\nu(\text{TMPC})]^{1/2}$. The thermal expansion coefficients, $\alpha P = (1/V)(\partial V/\partial T)|_P$, are given at 200°C.

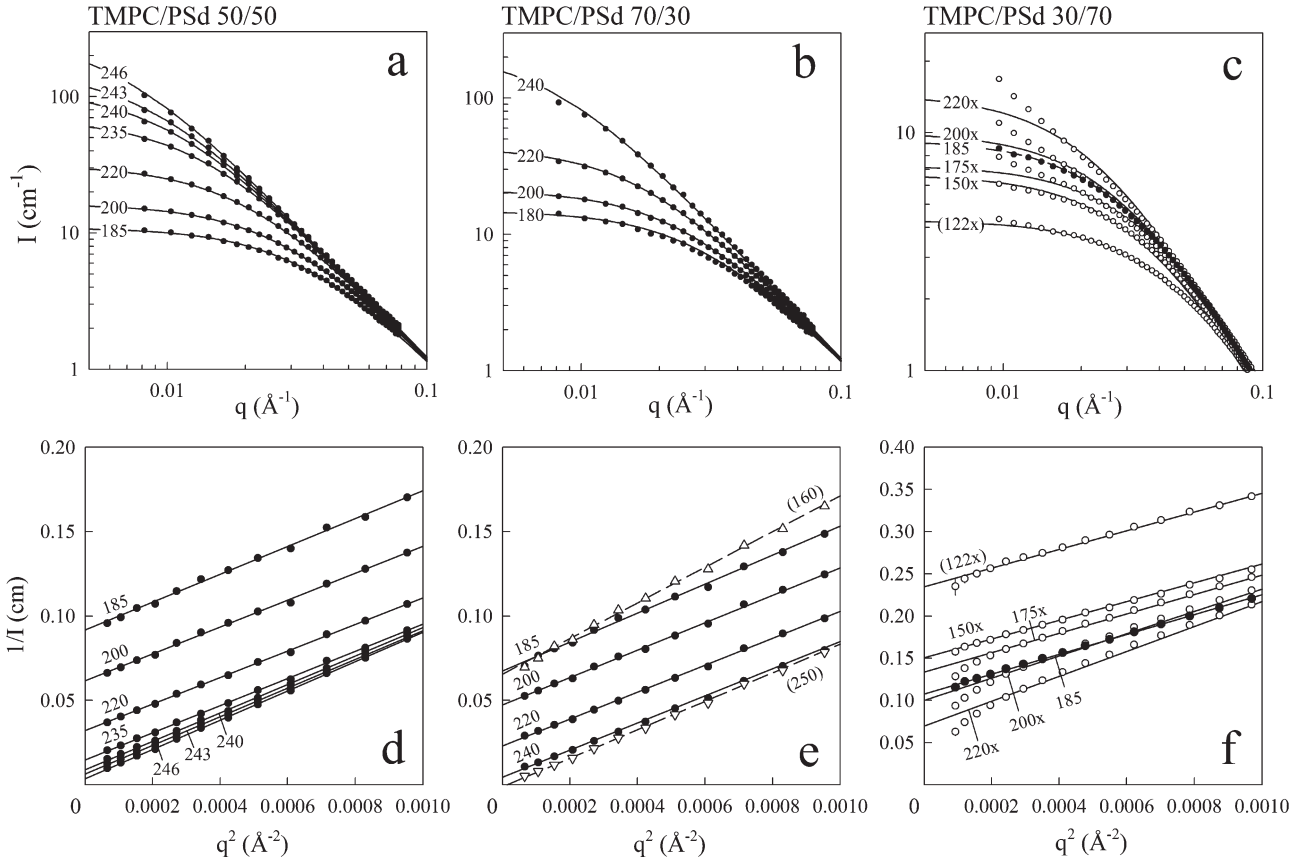

Figure 2. Coherent scattering intensity obtained for mixtures TMPC/PSd of composition (a) 50/50, (b) 70/30, and (c) 30/70 (mass fraction) for various temperatures (in °C) in the one-phase region. The lines correspond to RPA fits according to eqs 2−5) with two adjustable parameters: $\tilde{\chi}_{12}$ and a(TMPC). (d-f) corresponding Ornstein−Zernike fits, eqs 9−11, at small wavenumber. Selected temperatures shown for clarity: (a,b,d,e) PAXE (LLB) data from samples (●) annealed in situ. For comparison purposes, part e includes two data sets (Δ) of specimens out of equilibrium: 160 °C (one-phase, near the mixture's T_g) and 250 °C (just above T_S). The measurements shown for TMPC/PSd 30/70 (c,e) were obtained with spectrometer D22 from (○) quenched and (●) in situ annealed specimens at various temperatures. The excess scattering at low wavenumber of quenched samples is discussed in the text.

Three compositions were prepared for SANS experiments—TMPC/PSd 30/70, 50/50, and 70/30 mass fraction—and they were cast from 10% w/v toluene solutions onto glass coverslips. The solvent was evaporated under (10^{-1} mbar) vacuum during 4 weeks, while gradually increasing the temperature up to 20 K above the mixtures' T_g. Free-standing polymer discs (16 mm in diameter and 100 μm thick) were peeled off the glass substrate. To obtain (solvent-free) samples of 1 mm thickness, 10 films were stacked together and lightly pressed at T_g + 20 K and then wrapped in thin aluminum foil (20 μm thick). Accurate sample thickness were measured (Mitutoyo micrometer with 1 μm resolution) to calibrate the scattering data in absolute units (cm^{-1}).

Experiments were carried out using both quenched and in situ annealed specimens. The former are advantageous as thermal equilibration can be ensured, particularly close to T_g, and since sample degradation can be minimized under vacuum (of TMPC in particular) by avoiding prolonged heating. Annealing temperatures and times were, respectively 130, 150, 175, 200, and 220 °C at 3 h, 2 h, 45 min, 25 min, and 10 min, estimated from light scattering kinetics.[33] The specimens were then rapidly quenched below T_g by contact with a large thermal mass cooled to 4 °C, in order to "freeze" concentration fluctuations at the annealing temperature. In situ heated samples must be equilibrated online but, in contrast, do not require quenching, which may cause artifacts due to length scale-dependent thermal equilibration.[34,35]

The phase diagram of TMPC/PSd was previously measured by light scattering experiments and observed to shift upward by 10−15 °C with respect to hydrogenous TMPC/PS.[19,20,33] Deuterium labeling is known to shift mixture phase boundaries, caused by a small difference in segment volume in hydrogenous and deuter-

ated polymers first pointed out by Buckingham and Hentschel[36] and reported for numerous mixtures (reviewed in ref 26).

B. Small Angle Neutron Scattering. Three series of experiments were performed at different small-angle neutron scattering diffractometers: (a) D22 (Institute Laue-Langevin, Grenoble, France), using an incident neutron wavelength of $\lambda = 8$ Å, 11.2 m collimation and a sample−detector distance of $D_{s-d} = 5.043$ m, which covers a wavenumber range of $0.0096 < q < 0.103$ Å^{-1}; (b) PAXE (Laboratoire Léon Brillouin, Saclay, France) configured to $\lambda = 6$ Å, a diaphragm collimation ($\phi_1 = 9$ mm, $\phi_2 = \infty$, and $\phi_3 = 15$ mm) and $D_{s-d} = 5.094$ m, yielding $0.0082 < q < 0.078$ Å^{-1}; (c) LOQ (ISIS, Oxfordshire, U.K.), operating at 25 Hz repetition rate, with a polychromatic $\lambda = 2-10$ Å, incident beam and $D_{s-d} = 4$ m, resulting in a very large (but fixed) wavenumber dynamic range $0.009 < q < 0.249$ Å^{-1}. The elastic wavenumber is

$$q = \frac{4\pi}{\lambda}\sin\left(\frac{\theta}{2}\right) \approx \frac{2\pi}{\lambda}$$

for small scattering angles θ.

An automatic sample changer was used for experiments on preannealed specimens while scattering from mixtures at equilibrium were acquired using an *in situ* heating "kinetics" cell. The custom-made "*T*-jump" cell consists of two brass ovens with quartz windows and a motorized sample carrier, described elsewhere.[33] Acquisition times varied from 10 min, for TMPC/PSd mixtures, to 1 h, for backgrounds, water and empty cells.

After (i) empty cell subtraction, the centrosymmetric raw spectra were (ii) radially averaged, (iii) normalized using the isotropic scattering of (1 mm) water, and (iv) calibrated with a set of secondary standards and direct beam.[33] The coherent scattering function was obtained after subtraction of the appropriate volume fraction of the calibrated spectra of the pure components, TMPC and PSd. Scattering from the latter is negligible compared the incoherent contribution of TMPC.

Sample thicknesses, necessary for absolute intensity calibration, were determined independently by (i) direct measurement with a micrometer and (ii) from the specimen transmission and calibration curve (transmission vs thickness) for selected neutron wavelengths (6 and 8 Å).[33] Uncertainties, of the order of 5%, were computed into final scattering intensities.

IV. Results and Discussion

A. RPA Analysis. The coherent scattering function of mixtures TMPC/PSd 50/50, 70/30, and 30/70 mass fraction as a function of temperature in the one-phase region is shown in Figure 2. The lines correspond to RPA fits, taking polysdispersity into account, according to eqs 1−4) with two adjustable parameters: χ_{12} and segment length a(TMPC) (as a(PS) is precisely known[37]. The corresponding Ornstein−Zernike (OZ) fits (eq 9−11, at small wavenumber) are shown in parts d−f. The filled symbols correspond to spectra of specimens annealed in situ while open symbols correspond to "quenched" samples.

RPA is found to describe all equilibrium, one-phase, experimental data remarkably well. Similarly, in the OZ representation, single-phase scattering appears as parallel lines of constant slope (indicating constant polymer dimensions) and positive intercept (proportional to G''), as expected from eqs 9−11.

Excess forward scattering is observed in Figure 2c,f for the TMPC/PS 30/70 blend for quenched samples and is absent in the *in situ* annealed blend (filled symbols). This is associated with nonequilibration and is discussed in section IV.B. Similarly, selected TMPC/PSd 70/30 spectra (open symbols) exhibit unusual OZ plots, specifically showing a larger slope for the lowest temperature (160 °C) or a negative intercept at 250 °C. The former is within ≈ 10 °C ofthe glass transition T_g and out of equilibrium at annealing times utilized; the latter is above the spinodal temperature T_s for the mixture, hence undergoing phase separation. Such nonequilibrium measurements are therefore excluded from the RPA or OZ analysis.

The RPA parameters obtained are shown in Figure 3 the effective interaction parameter $\tilde{\chi}_{12}/v_0$, the second derivative of the free energy G'' and the correlation length of composition fluctuations ξ, as a function of temperature for three compositions. The extrapolation of parameters to $G'' \rightarrow 0$, $\tilde{\chi}_{12}/v_0 \rightarrow \chi_s/v_0 \rightarrow$ and $\xi \rightarrow \infty$ at the spinodal, provides a direct measure of the spinodal location. For the TMPC/PSd 50/50 mixture, we obtain $G'' = 1.164/T - 0.00223$,

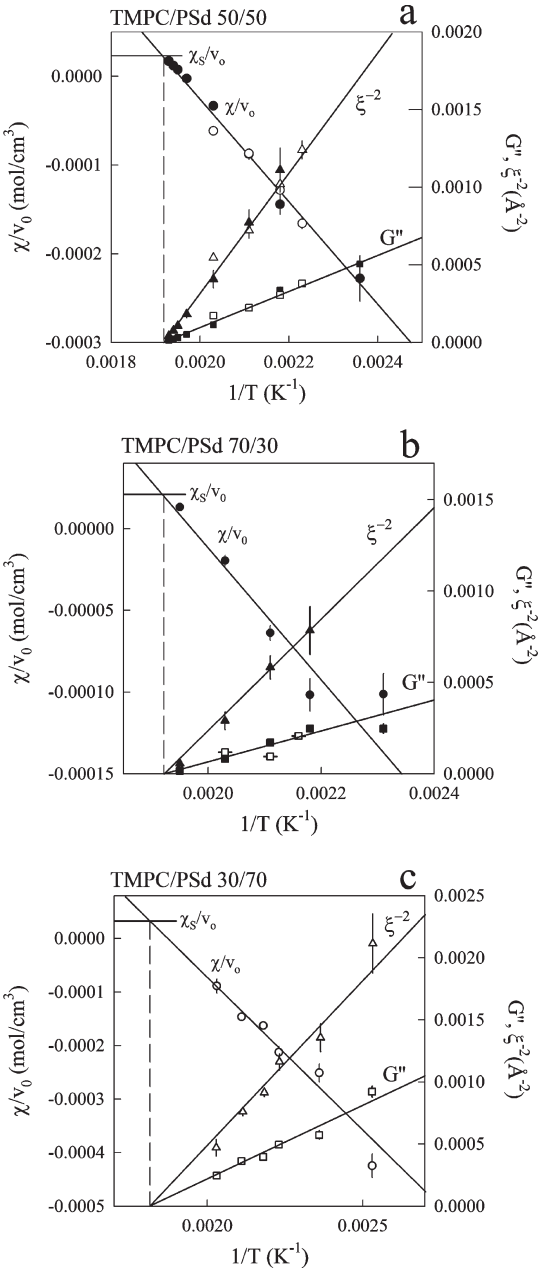

Figure 3. Random phase approximation (RPA) parameters obtained from fits to scattering data obtained using instruments PAXE, D22 and LOQ: (●, ○) effective interaction parameter $\tilde{\chi}_{12}/v_0$; (■, □) second derivative of the free energy G''; (▲, Δ) correlation length of composition fluctuations ξ, as a function of temperature. Closed and open symbols correspond to *in situ* and quenched mixtures, respectively. Calculated spinodal $\tilde{\chi}_{S12}/v_0$ and temperature T_S are indicated by solid and dashed lines, respectively.

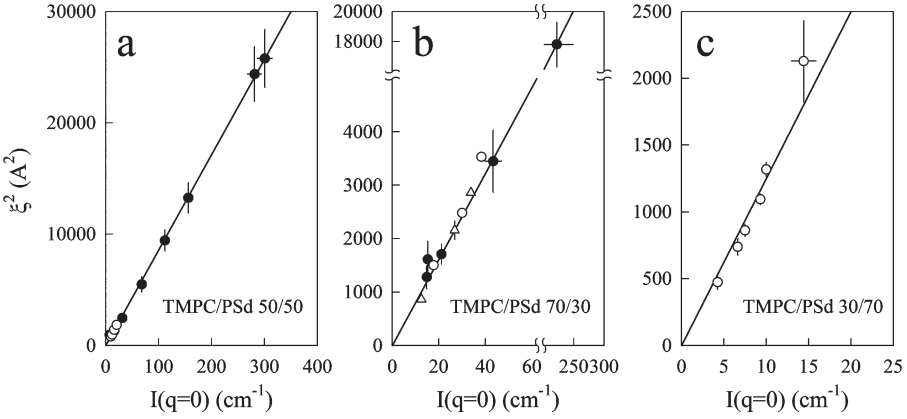

Figure 4. RPA self-consistency test: correlation length squared ξ^2 versus zero-angle scattering $I(o) = kS(q = 0)$. Measurements from samples annealed in situ (●, PAXE) and quenched to room temperature (○, D22 and Δ, LOQ). The linear dependence expected from eqs 9−11 is observed for all mixtures, in contrast with earlier report of RPA deviations.[11]

$\tilde{\chi}_{12}/v_0 = -0.578/T + 0.00113$ mol/cm^3 [$\chi_s/v_0 = 2.277 \times 10^{-5}$ mol/cm^3], and $\xi^{-2} = 3.85/T - 0.00738$ Å^{-2}. The spinodal temperature was (independently) extrapolated to yield $T_s(50/50) \approx 249 \pm 2$ °C.[38] The following parameters are obtained for off-critical mixtures: TMPC/PSd 30/70 yields $G'' = 1.18/T - 0.00214$, $\tilde{\chi}_{12}/v_0 = -0.547/T + 0.00102$ mol/cm^3[$\chi_s/v_0 = 3.257 \times 10^{-5}$ mol/cm^3], and $\xi^{-2} = 2.53/T - 0.00457$ Å^{-2}, yielding $T_s(30/70) \approx 285 \pm 10$ °C (the larger uncertainty arises from the extrapolation further away from experimental data, prevented by degradation). Finally, for TMPC/PSd 70/30, we obtain $G'' = 0.83$/T - 0.0016, $\tilde{\chi}_{12}/v_0 = -0.404/T + 0.000796$ mol/cm^3 [$\chi_s/v_0 = 2.09 \times 10^{-5}$ mol/cm^3], and $\xi^{-2} = 3.053/T - 0.00587$ Å^{-2}, yielding $T_s(70/30) \approx 248 \pm 1$ °C.

Results for the spinodal temperatures of all mixtures are good agreement with phase separation data from both neutron and light scattering experiments,[39] independently corroborating the accuracy of the one-phase measurements.

RPA theory predicts a correlation between the forward scattering $S(0)$ and the correlation length given by

$$\xi \equiv \sqrt{AS(0)}$$

(cf. eqs 9−11). A representation of ξ^2 as a function of $S(0)$ is therefore expected to be linear if RPA holds. Figure 4 plots the relationship between ξ^2 and $I(q = 0)$, the forward scattering intensity, which are two quantities independently determined from the data: the first is proportional to the OZ slope and the second is the inverse intercept.[40]. This plot is an important self-consistency check for the RPA and its nonlinearity has been associated previously to the spatial dependence of the χ parameter. Measurements reported by Brereton, Fischer and co-workers (cf. ref 11, Figure 3) appear to indicate a nonzero intercept of this linear relationship and an unusually large slope in comparison with other mixtures (described approximately by $\xi^2 \approx 7000 \pm 180I(0)$ Å^2). In contrast, our results show remarkable agreement between mean-field theory and experiment. We find well-behaved relationships, with zero intercept, for all compositions, given by $\xi^2(50/50) = 85.8\ I(0)$, $\xi^2(30/70) = 125\ I(0)$, $\xi^2(70/30) = 80.4\ I(0)$ Å^2.

On the basis of the experimentally observed nonlinearity, Brereton et al.[11] proposed that the RPA could not account for the scattering of this mixture and proposed an extension of this formalism assuming a spatially dependent $\chi(r)$. The *thermodynamic* nature of the Flory χ parameter, governed by monomer−monomer contact interactions, is expected to yield a structureless χ for length scales above ~ Kuhn length, for which mean-field theory holds. The proposed spatial dependenceof χ observed in TMPC/PSd caused much controversy in the literature for decades. The current work should settle this controversy as exhaustive experiments on three spectrometers, considering various compositions and an unprecedented temperature range, show no evidence of anomalies in the single-phase equilibrium measurements. The following section discusses nonequilibrium effects in scattering from concentration fluctuation in mixtures that may give rise to the previously reported "anomalies".

B. Nonequilibrium and "Apparent" Spatial Dependence of χ. Scattering from mixtures out of equilibrium are generally identified by some time dependence of the spectra. However, this evolution can be slow or imperceptible for high molecular weight polymers close to, or below, the glass transition temperature T_g (such as quenched specimens). Nonequilibrium anomalies include (i) phase-separation, (ii) noninstantaneous quenching, (iii) voids, and (iv) additional processes (e.g., crystallization).

(i) Phase separating mixtures scatter strongly in the forward direction. In the OZ representation, phase separation results in curved S^{-1} vs q^2 plots, with an apparent steeper low-q slope and a negative intercept (yielding an unphysical $\xi < 0$). The latter can only be observed if sufficiently low q is measured, illustrated in Figure 2e for TMPC/PSd 70/30 annealed only 2 °C inside the spinodal boundary, exhibiting a nonparallel OZ slope and a small negative intercept. Figure 5 depicts a deeper quench to 260 °C (▽, 12 °C inside spinodal T_s) for a TMPC/PSd 50/50 mixture. The solid lines represent equilibrium scattering functions, obtained in Figure 2d, included for comparison.

(ii) Noninstantaneous quenching from a certain annealing temperature T_i to below T_g can generate more subtle artifacts, as the relaxation of concentration fluctuations is wavelength dependent, as expected from Cahn−Hilliard−Cook theory.[41] Short wavelength fluctuations (high q) equilibrate faster than long wavelength (low q) fluctuations which require diffusion over large length scales. As a result, a "slowly" quenched sample retains memory of its original temperature fluctuations at low-q but may equilibrate at higher q to its "new" temperature. Scattering from such specimens may exhibit strong deviations from RPA, dominated by thermal history. Figure 5 shows a time series of scattering from a TMPC/PSd 50/50 specimen, initially equi-

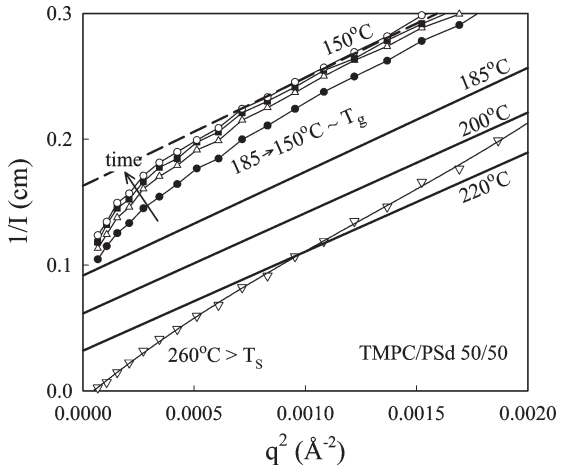

Figure 5. Nonequilibrium structure factors and consequences to OZ analysis illustrated with TMPC/PSd 50/50 measurements at various temperatures (PAXE). Solid lines are selected equilibrium scattering functions (from Figure 2d), for comparison purposes. Measurements inside the phase boundary (▽): unstable quench to 260 > T_S. Phase separation results in nonlinear $S^{1-}(q^2)$, with an apparent steeper slope A and a negative intercept (and hence "negative" ξ). Nonequilibrium measurements within the one-phase region: temperature jump from 185 to 150 °C (T_g+20 °C) at time intervals (●) 0−2 h, (Δ) 2−4 h, (■) 4−6 h, and (○) 6−6 h 40 min. Nonlinearity emerges due to slower equilibration of large wavelength (low q) composition fluctuations. Dashed line is an estimated equilibrium structure factor obtained for 150 °C by extrapolation from high temperature data (from Figure 2a).

librated at 185 °C and annealed isothermally at 150 °C (approximately 20 °C above T_g). After annealing for 7 h, the long wavelength composition fluctuations has still not reached equilibrium, resulting in a curved OZ plot. However, the expected OZ behavior was already visible at higher q. Nonequilibrium scattering functions are often "pinned" at low and high q by, respectively, the "original" and "final" temperature scattering functions.

Quenching below T_g often results in similar nonlinearities as shown in Figure 2f for TMPC/PS 30/70 in which all quenched spectra (open symbols) exhibit excess scattering, but in situ annealed specimens (185 °C, filled symbols) do not. Very large excesses have been observed by Maconnachie et al.[34] in mixtures of PS/PPO and P4MS/PPO and related to nonequilibration of samples.

(iii) Homogeneous polymers and mixtures may also exhibit excess forward (low-q) intensity and scattering caused by voids or surface roughness (in addition to expected density fluctuations), which depend critically on sample preparation.[42−46] In our work, both TMPC and PSd show some excess forward scattering, of the order of 1−3 cm^{-1},[33] but which is small with respect to 10−100 cm^{-1} signal of mixture concentration fluctuations. Such backgrounds are nevertheless subtracted from the mixture data in the appropriate volume fractions.

(iv) Finally, concurrent processes such as crystallization or solvent/moisture-induced separation can, of course, result in additional scattering. TMPC has been reported to crystallize over long times above 200 °C[13] and must be checked by calorimetry. Also, miscibility gaps occur in ternary polymer−solvent mixtures (e.g., TMPC/PC/CH_2Cl_2[47]) caused by solvent quality asymmetry, which may be crossed during sample drying from solution casting.

Definitive conclusions regarding the observations reported previously[11] would require exact knowledge of sample preparation and thermal history. However, based on the present results, we propose that noninstantaneous quenching is probably responsible for the excess forward scattering, as deviations are observed mainly at the highest temperatures and concern rather low wavenumbers (0.007 < q < 0.024 $Å^{-1}$).

C. Kratky Asymptote and Segment Length. The structure factor of a homogeneous mixture at high wavenumber becomes greatly simplified. When $qR_g \gg 1$, the Gaussian form factor (eq 4) becomes

$$\langle g_D(x)\rangle_w \approx \frac{2}{x} \equiv \frac{2}{q^2\langle {R_g}^2\rangle_n} \tag{12}$$

which can be replaced in eq 2 to give

$$S(q) \approx \frac{12\phi_1\phi_2}{q^2}\frac{v_0}{\hat{a}^2} \tag{13}$$

where an "apparent" or "average" statistical length $\hat{a}$ is now defined by

$$\frac{\hat{a}^2}{v_0} \equiv \phi_1\phi_2\left(\frac{{a_1}^2}{\phi_1 v_1} + \frac{{a_2}^2}{\phi_2 v_2}\right) \tag{14}$$

which does not depend on the molecular weight distribution (unlike its low angle counterpart in eqs 9−11). In the case of an isotopic mixture of polymers of a certain segment length a (for example, refs 44 and 48 and references therein), eq 13 retains its form[49]

$$S(q) \approx \frac{12\phi_1\phi_2 v}{q^2 a^2}$$

hence the definition chosen for $\hat{a}$. Therefore, the statistical repeat length can be determined directly from the high-q asymptote of scattering data. A Kratky plot (Iq^2 vs q) is frequently used for this purpose, yielding a q-independent plateau at large q. However, the determination of such plateau depends critically on an accurate subtraction of the incoherent scattering background with due consideration to its temperature dependence and volume of mixing. At even higher q values, rod-like features appear (in particular for chains with important lateral dimensions), and a departure from the flat asymptote occurs. Therefore, the q window of the structure factor where the intensity decays with q^2 is roughly limited to $5{R_g}^{-1} < q < a^{-1}$; i.e., the scale probed must be smaller than the radius of gyration but larger than the segment (or Kuhn) length.

Figure 6 depicts the Kratky plots of all three mixtures at various temperatures. The LOQ diffractometer provides a particularly useful q-range for such measurements, as it reaches nearly 0.25 Å (albeit with limited statistics) due to its polychromatic incident beam. We obtain segment Kratky asymptotes and uncertainties for all data, which are then plotted in Figure 7a. In order to increase the accuracy of the measurement of the segment length of TMPC, we fix the well-known PS segment length to a(PS) = 6.7 Å.[37,43,50] The solid lines correspond to eq 13 computed at two extreme temperatures studied, taking volume changes into account, and fit the data remarkably well, resulting in a segment length a(TMPC) = 20.1 ± 0.9 Å. To our knowledge, this is the first determination of the segment length of TMPC.

Separately, Figure 7b plots the Ornstein−Zernike slope A, at lower q and fully considering polydispersity, as a function of composition. The lines are plots of eq 11 which describe the data with the same parameters, corroborating the estimates above.

V. Interaction Parameter $\chi(\phi,T)$ and Previous Measurements

TMPC is the only known polycarbonate miscible with polystyrene.[14,16,51] TMPC/PS exhibit marginally negative volumes of mixing at all compositions[14,52] and no obvious mechanical synergy.[52] However, TMPC/PS may be considered a highly interactive mixture, based on the magnitude of its χ parameter-dependence in temperature (i.e., $|B|$ in the usual Flory−Huggins $\chi = A + B/T$).[26] Previous χ parameter estimates include FRES bilayer diffusion measurements,[17,25] SANS (as a function of composition),[24] and equation of state theory, based on phase boundaries determined optically.[18,53] The present measurements and previously reported $\chi(\phi,T)$ are summarized in Figure 8 and discussed below. All $\tilde{\chi}_{12}/v_0$ were referenced to $v_0 = 175\ \text{cm}^3/\text{mol}$, for comparison purposes.

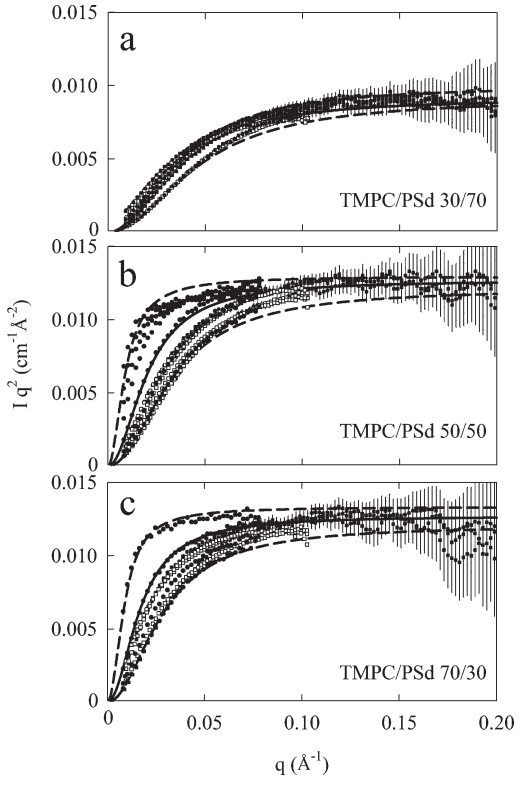

Figure 6. Kratky plots of TMPC/PSd 30/70, 50/50 and 70/30 (w/w) static structure factors, at all studied temperatures, obtained at (■) LOQ, (□) D22, and (○) PAXE. The lines correspond to RPA theory adjusting solely the segment length a(TMPC) while fixing well-known a(PS) = 6.7 Å.[37] Note that the Kratky plateau is independent of the polydispersity. The solid and dashed lines indicate, respectively, the most probable and the upper/lower limits of a(TMPC) compatible with the data (computed at extreme temperatures of data): (a) 19.7 ± 0.9 Å, (b) 19.9 ± 0.6 Å, and (c) 20.3 ± 1 Å.

Yang and O'Reilly[24] reported SANS measurements of TMPC/PSd as a function of composition at constant temperature. Five mixtures of different composition were annealed at $T(\phi) = T_g(\phi) + 50$ °C, quenched and measured at room temperature. The $\chi(\phi)$ parameters obtained (○) are in excellent agreement in the current results (●), as shown in Figure 8a.

Kramer and co-workers have measured tracer[25] and mutual[17] diffusion coefficients of thin films bilayers (200−400 nm) of deuterium labeled TMPC and PS, annealed in the one-phase region, using depth profiling by FRES. Monomer friction coefficients were obtained by varying the molecular weights of both tracer and matrix polymers, according to the reptation model[25]. Mutual diffusion coefficients were measured from interdiffusion profiles of bilayers of mixtures of similar composition annealed below the LCST.[17] χ parameters were then computed from mutual and tracer diffusion results, using an Onsager transport coefficient given by the "fast theory". The procedure assumes that mutual diffusion is governed by enthalpy and noncombinatorial terms of the free energy of mixing, thereby defining χ, while tracer diffusion is driven solely by combinatorial entropy of mixing. The composition dependence of χ at $T = T_g + 45$ °C is shown in (□) Figure 8a and $\chi(T)$ for two mixtures, TMPC/PSd 75/25 and 50/50 (w/w) are shown in Figure 8b.[17] The FRES measurements agree relatively well at high TMPC concentrations ($\phi > 0.5$) but differ considerably at low concentrations, albeit with large uncertainties. FRES results appear to overestimate the slope of $\chi(50/50,T)$ and underestimate $\chi(75/25,T)$ but are in accord with SANS measurements about their relative magnitude. Supported films of TMPC/PSd on nativesilicon oxide are known to undergo asymmetric attraction, with PSd and TMPC segregating to the air and silicon interfaces, respectively.[54] For this reason, PSd, the component with lower surface-air energy, was chosen as the bilayer top film. Complications arising from competing surface attraction (which causes eventually surface directed spinodal decomposition[54]) could be responsible for the discrepancies, as well as the rather complex multiparameter fitting.

Sanchez−Lacombe lattice fluid theory was also employed to estimate $\chi(\phi, T)$.[18,53] The equation of state approach (Δ) predicts reasonable magnitudes for the interaction parameter but does not agree quantitatively on the composition nor temperature dependence of the χ parameter. However, all experimental and predicted spinodal temperatures agree rather well, with the exception of ES2000,[18] which overestimates the experimentally observed T_S.

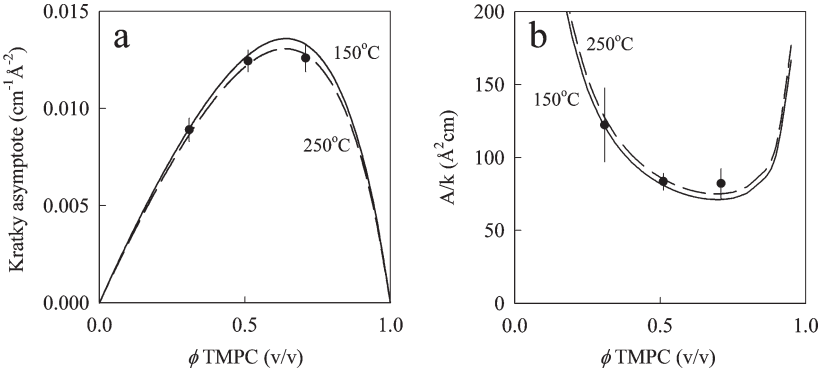

Figure 7. SANS determination of the segment length of TMPC. (a) Kratky asymptote as a function of composition. Lines are calculations of eqs 13 and 14 for the two temperature extremes 150−250 °C. (b) Ornstein−Zernike experimental slopes A [Åcm] as a function of composition, extracted from Figure 2, fitted to eq 11. Note that A but not the Kratky plateau depends on the molecular weight distribution (obtained by GPC) of the components. Both procedures yield a(TMPC) = 20.1 ± 0.9 Å.

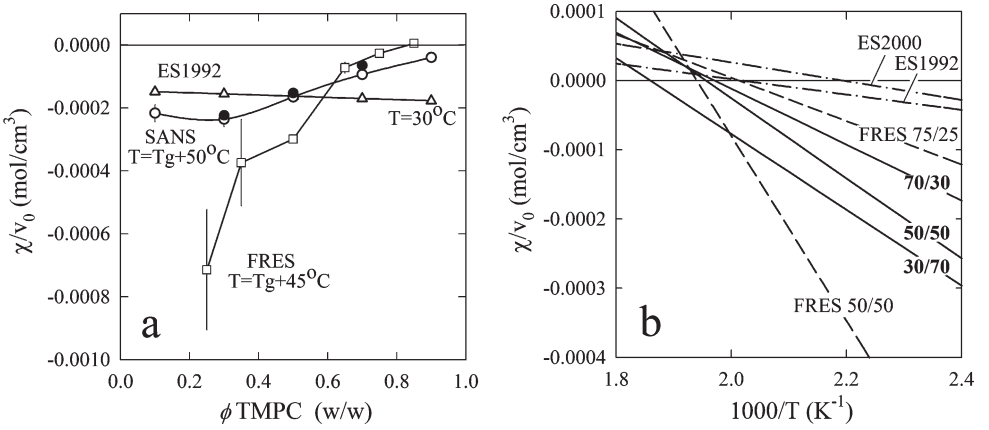

Figure 8. (a) Composition dependence of $\tilde{\chi}_{12}/v_0$ obtained by SANS [(●) current work and (○) ref 24], (□) FRES[17] and (Δ) predicted by equation of state theory[18,53]. (b) Temperature dependence of $\tilde{\chi}_{12}/v_0$, referenced to $v_0 = 175$ cm^3/mol, obtained by the various methods (ES computed for 50/50 composition).

Finally, we compare the current findings for the temperature dependence of χ with other mixtures, following the compilation by Balsara[26]. We consider LCST mixtures with $\chi = (A + B/T)/v_0$ and use a common reference volume $v_0 = 100$ Å^3. In particular, we focus on the slope parameter B, which is taken as measure of the interaction *strength*. We obtain B/v_0 for TMPC/PSd 30/70, 50/50, and 70/30 of respectively −36.7, −38.3, and −27.8 K/100 Å^3 (in contrast with FRES results of −80.7 and −18.7 K/100 Å^3 for TMPC/PSd 50/50 and 75/25). Other common mixtures exhibit B/v_0(PSd/PVME) = −41.6 K/100 Å^3, B/v_0(PI/PBd) = −0.9 to −3.2 K/100 Å^3. TMPC/PSd has therefore a relatively large normalized interaction parameter (although not the largest, as previously tabulated[26]) with a rather small composition dependence.

VI. Conclusions

We investigate the thermodynamics and chain dimensions of a highly interacting polymer mixture TMPC/PSd, as a function of temperature and composition, by small angle neutron scattering (SANS). In contrast with a previous controversial report,[11] we demonstrate that the random phase approximation (RPA) and a structureless, "point-like" $\chi(\phi,T)$ parameter describe all scattering data remarkably well.

The forward scattering of two component systems is directly proportional to their osmotic compressibility which, in turn, yields a scalar thermodynamic χ parameter according to de Gennes RPA.[9] Naturally, at sufficiently small length scales (typically $q > a^{-1}$) local effects emerge, normally accompanied by a departure from the Kratky asymptote[10] which is somewhat difficult to observe in flexible Gaussian chains as the scattering signal ($\sim q^{-2}$), incoherent (T dependent) background scattering and noise become comparable. Integral equation theories, such as the PRISM formalism,[55−57] compute direct local correlations between (monomeric or segmental) units. Incidentally, the resulting scattering for binary mixtures *can* be computed in a form mathematically similar to RPA eq 2 by invoking a q-dependent χ parameter. This *can* be associated with spatially dependent interactions as proposed earlier by Brereton et al.[11] to reconcile previous observations in TMPC/PSd.

We unequivocally show that scattering from TMPC/PSd is well described by RPA and that apparent deviations reported earlier were likely caused by nonequilibration of mixtures undergoing temperature jumps within the one-phase region, resulting in a wavelength-dependent relaxation of concentration fluctuations (in addition to trivial phase separation). The current exhaustive study should settle the controversy regarding the *experimental observations* and the need for a spatially dependent $\chi(q)$ to describe the scattering function of the mixture. While local correlations undoubtedly exist at the segmental-scale and integral equation theories such as PRISM are powerful means of estimating them, we question the validity and usefulness of their incorporation in an already overloaded χ parameter[11,55−58] which is often considered ϕ, M_w, and microstructure dependent.[26,59,60]

After demonstrating regular RPA behavior of TMPC/PSd, we determine interaction parameters $\chi(\phi,T)$ of this strongly interacting polymer mixture and the chain segment length for TMPC.

Acknowledgment. The authors thank EPSRC for funding and the Institute Laue-Langevin (Grenoble, France), the Laboratoire Léon Brillouin (Saclay, France) and the ISIS pulsed source (Oxfordshire, U.K.) for beamtime. We acknowledge José Teixeira (LLB), Ferdinando Formisano (ILL), Isabelle Grillo (ILL), and Steve King (ISIS) for assistance and many useful discussions and Randall Richards (RC-UK, Durham University) for donating the deuterated polystyrene specimen.

References and Notes

(1) Olabisi, O.; , Robertson, L. M.; , Shaw, M. *Polymer-polymer miscibility*; Academic Press: New York, 1979.
(2) Cowie, J. M. G. *Polymers: Chemistry and Physics of Modern Materials*, 2nd ed., Blackie Academic and Professional: London, 1991.
(3) Flory, P. J. *J. Chem. Phys.* **1941**, *9*, 660.
(4) Flory, P. J. *J. Chem. Phys.* **1942**, *10*, 51.
(5) Huggins, M. *J. Chem. Phys.* **1941**, *9*, 440.
(6) Flory, P. J. *Discuss. Faraday Soc.* **1970**, *49*, 7.
(7) Sanchez, I. C. In *Polymer blends*; Paul, D. R., Newman, S., Ed.; Academic: New York, 1978. Chapter 3, p 115.
(8) Sanchez, I. C.; Balazs, A. C. *Macromolecules* **1989**, *22*, 2325.
(9) P.-G. de Gennes. *Scaling concepts in polymer physics*; Cornell University Press: Ithaca, NY, 1979.
(10) Higgins, J. S.; Benoit, H. C. *Polymers and neutron scattering*; Clarendon Press: Oxford, U.K., 1994.
(11) Brereton, M. G.; Fischer, E. W.; Herkt-Maetzky, Ch.; Mortensen, K. *J. Chem. Phys.* **1987**, *87*, 6144.
(12) Casper, R.; Morbitzer, L. *Angew. Makromol. Chem.* **1977**, *58*, 1.
(13) Illers, K.-H.; Heckmann, W.; Hambrecht, J. *Colloid Polym. Sci.* **1984**, *262*, 557.
(14) Fernandes, A. C.; Barlow, J. W.; Paul, D. R. *Polymer* **1986**, *27*, 1788.
(15) Guo, W.; Higgins, J. S. *Polymer* **1990**, *31*, 699.
(16) Kim, C. K.; Paul, D. R. *Macromolecules* **1992**, *25*, 3097.
(17) Kim, E.; Kramer, E. J.; Osby, J. O.; Walsh, D. J. *J. Polym. Sci., Polym. Phys. Ed.* **1995**, *33*, 467.
(18) Merfeld, G. D.; Paul, D. R. *Polymer* **2000**, *41*, 649.
(19) Cabral, J. T.; Higgins, J. S.; McLeish, T. C. B.; Strausser, S.; Magonov, S. N. *Macromolecules* **2001**, *34*, 3748.

(20) Cabral, J. T.; Higgins, J. S.; Yerina, N. A.; Magonov, S. N. *Macromolecules* **2002**, *35*, 1941.
(21) Binder, K.; Frisch, H. L.; Jäckle, J. *J. Chem. Phys.* **1986**, *85*, 1505.
(22) Schwahn, D.; Mortensen, K.; Springer, T.; Yee-Madeira, H.; Thomas, R. *J. Chem. Phys.* **1987**, *87*, 6078.
(23) Janssen, S.; Schwahn, D.; Springer, T. *Phys. Rev. Lett.* **1992**, *68*, 3180.
(24) Yang, H.; O'Reilly, J. M. *Mater. Res. Soc. Symp. Proc.* **1987**, *79*, 129.
(25) Kim, E.; Kramer, E. J.; Osby, J. O. *Macromolecules* **1995**, *28*, 1979.
(26) Balsara, N. P. Thermodynamics of polymer blends. In *Physical Properties of Polymers Handbook*; Mark, J. E., Ed.; AIP Press: Woodbury, NY, 1996; p 257.
(27) The reference molar volume can also be defined as an arithmetic mean, $v_0 = (\phi_1 v_1 + \phi_2 v_2)$, or a harmonic mean, $1/v_0 = (\phi_1/v_1 + \phi_2/v_2)$ of the component molar volumes (for example, see refs 44 and 61−63). We have chosen a geometric mean for consistency with previously published literature.
(28) The polydisperse form factor can be written as[62,64−66]

$$g_D(x) = \frac{2}{(1+1/h)x^2}\left[\left(1+\frac{x}{h}\right)^{-h} - 1 + x\right]$$

where x and h are defined in eq. (4). It is related to its weight average (eq 4) by $\langle g_D(x)\rangle_w = \langle N\rangle_w/\langle N\rangle_n\, g_D(x)$. Note that, while $g_D(x)$ is normalized to 1, this weight average is normalized to the polydispersity index. At small wavenumber the weight-average form factor becomes[62,64]

$$\langle g_D(R_{gi}{}^2 q^2)\rangle_w \approx \frac{\langle N\rangle_w}{\langle N\rangle_n}\left[1 - \frac{\langle N\rangle_z}{3\langle N\rangle_n}\langle R_g^2\rangle Nq^2\right] = \frac{\langle N\rangle_w}{\langle N\rangle_n}\left[1 - \frac{\langle R_g{}^2\rangle_z q^2}{3}\right]$$

(29) Schultz, G. V. *Z. Phys. Chem., Abt. B* **1939**, *43*, 25.
(30) Zimm, B. H. *J. Chem. Phys.* **1948**, *16*, 1099.
(31) Linear but also polynomial $\chi(T)$ relationships are found experimentally and a useful compilation of $\chi(T)$ is given in ref 26.
(32) Tetramethyl bisphenol A polycarbonate (tmpc) stands for poly(oxycarbonyloxy(2,6-dimethyl-1,4-phenylene)isopropylidene(3,5-dimethyl-1,4-phenylene)).
(33) Cabral, J. T. Ph.D. Thesis, Imperial College, London, **2002**.
(34) Maconnachie, A.; Fried, J. R.; Tomlins, P. E. *Macromolecules* **1989**, *22*, 4606.
(35) Maconnachie, A. *Polymer* **1984**, *25*, 1068.
(36) Buckingham, A. D.; Hentschel, H. G. E. *J. Polym. Sci., Polym. Phys. Ed.* **1980**, *18*, 853.
(37) Londono, J. D.; Narten, A. H.; Wignall, G. D.; Honnell, K. G.; Hsieh, E. T.; Johnson, T. W.; Bates, F. S. *Macromolecules* **1994**, *27*, 2864.
(38) We performed this analysis assuming constant volumes and verified that the differences are of the order of the experimental uncertainty; The following monomer molar volumes were used: v(PS) = 99.19 and v(TMPC) = 286.34 cm^3/mol (corresponding to ρ(PSd) = 1.13 and ρ(TMPC) = 1.084 g/cm^3) and reference v_0 = 175 cm^3/mol (for consistency with the literature) at all temperatures. Slightly steeper temperature dependences are found, namely $G'' = 1.300/T - 0.00249$, $\tilde{\chi}_{12}/v_0 = -0.636/T + 0.00124$ mol/cm^3, $= \tilde{\chi}_{12} - 111.3/T + 0.217$, and $\xi^{-2} = 3.62/T - 0.00692$. At the spinodal, we obtain $\chi_s/v_0 = 2.479 \times 10^{-5}$ mol/cm^3 (or $\chi_s = 4.34 \times 10^{-3}$). The spinodal temperatures obtained are within 250.1 and 251.7 °C, in good agreement with the more accurate temperature-dependent density analysis presented.
(39) Cabral, J. T.; Higgins, J. S. Manuscript in preparation.
(40) The correlation length ξ remains constant regardless of whether we consider constant or temperature dependent molar volumes. the same applies to the relationship ξ^2 vs $I(q = 0)$, because both are directly determined experimentally. The experimental slope is $m \equiv A/k$, the zero-angle scattering intensity is $I(0) \equiv kS(0)$ and since the correlation length is given by

$$\xi^2 \equiv AS(0) = \frac{A}{k}[kS(0)] = mI(0)$$

it is independent of the contrast factor, k. The robustness of this relationship makes it a relevant coherence test of this analysis.
(41) Strobl, G. R. *Macromolecules* **1985**, *18*, 558.
(42) Boué, F.; Nierlich, M.; Leibler, L. *Polymer* **1982**, *23*, 29.
(43) Bates, F. S.; Wignall, G. D. *Macromolecules* **1986**, *19*, 934.
(44) Bates, F. S.; Fetters, L. J.; Wignall, G. D. *Macromolecules* **1988**, *21*, 1086.
(45) Clark, J. N.; Fernandez, M. L.; Tomlins, P. E.; Higgins, J. S. *Macromolecules* **1993**, *26*, 5897.
(46) Londono, J. D.; Wignall, G. D. *Macromolecules* **1997**, *30*, 3821.
(47) Hellmann, E. H.; Hellmann, G. P.; Rennie, A. R. *Colloid Polym. Sci.* **1991**, *269*, 343.
(48) Bates, F. S.; Muthukumar, M.; Wignall, G. D.; Fetters, L. J. *J. Chem. Phys.* **1988**, *89*, 535.
(49) An alternative definition of $S(q)$ is commonly preferred for isotopic mixtures:

$$\left.\frac{d\sigma}{d\Omega}(q)\right|_{coh} = N_a(b_1 - b_2)^2/\nu\, S(q)$$

where $s(q) \approx 12\phi_1\phi_2/q^2a^2$ is now dimensionless.
(50) Wignall, G. D. In *Encyclopedia of Polymer Science and Engineering*; Grayson, M., Kroachwitz, J., Eds.; Wiley: New York, 1987; Vol. *10*, p 112.
(51) Landry, C. J. T.; Yang, H.; Machell, J. S. *Polymer* **1991**, *32*, 44.
(52) Yee, A. F.; Maxwell, M. A. *J. Macromol. Sci. Phys.* **1980**, *B17*, 543.
(53) Kim, C. K.; Paul, D. R. *Polymer* **1992**, *33*, 1630.
(54) Kim, E.; Krausch, G.; Kramer, E. J.; Osby, J. O. *Macromolecules* **1994**, *27*, 5927.
(55) Schweizer, K. S.; Curro, J. G. *Phys. Rev. Lett.* **1988**, *60*, 809.
(56) Schweizer, K. S.; Curro, J. G. *J. Chem. Phys.* **1989**, *91*, 5059.
(57) Curro, J. G.; Schweizer, K. S. *Macromolecules* **1991**, *24*, 6736.
(58) Zirkel, A.; Gruner, S. M.; Urban, V.; Thiyagarajan, P. *Macromolecules* **2002**, *35*, 7375.
(59) Bidkar, U. R.; Sanchez, I. C. *Macromolecules* **1996**, *28*, 3963.
(60) Cui, S. T.; Cochran, H. D.; Cummings, P. T.; Kumar, S. K. *Macromolecules* **1997**, *30*, 3375.
(61) Hasegawa, H.; Sakurai, S.; Takenaka, M.; Hashimoto, T.; Han, C. C. *Macromolecules* **1991**, *24*, 1813.
(62) Sakurai, S.; Hasegawa, H.; Hashimoto, T.; Hargis, I. G.; Aggarwal, S. L.; Han, C. C. *Macromolecules* **1990**, *23*, 451.
(63) Sakurai, S.; Izumitani, T.; Hasegawa, H.; Hashimoto, T.; Han, C. C. *Macromolecules* **1991**, *24*, 4844.
(64) Joanny, J. F. *C. R. Acad. Sci., Paris* **1978**, *286B*, 89.
(65) Lapp, A.; Picot, C.; Benoit, H. *Macromolecules* **1985**, *18*, 2437.
(66) Mori, K.; Tanaka, H.; Hasegawa, H.; Hashimoto, T. *Polymer* **1989**, *30*, 1389.